Ab Initio Study of Graphene on SiC

Alexander Mattausch* and Oleg Pankratov

Theoretische Festkörperphysik, Universität Erlangen-Nürnberg, Staudtstrasse 7, 91058 Erlangen, Germany

(Received 8 January 2007; published 15 August 2007)

Employing density-functional calculations we study single and double graphene layers on Si- and C-terminated 1×1—$6H$-SiC surfaces. We show that, in contrast with earlier assumptions, the first carbon layer is covalently bonded to the substrate and cannot be responsible for the graphene-type electronic spectrum observed experimentally. The characteristic spectrum of freestanding graphene appears with the second carbon layer, which exhibits a weak van der Waals bonding to the underlying structure. For Si-terminated substrate, the interface is metallic, whereas on C face it is semiconducting or semimetallic for single or double graphene coverage, respectively.

DOI: 10.1103/PhysRevLett.99.076802 PACS numbers: 73.20.−r, 68.35.Ct, 68.47.Fg, 71.15.Mb

Recent years have witnessed an explosion of interest in the prospect of graphene-based nanometer-scale electronics [1–6]. Graphene, a single hexagonally ordered layer of carbon atoms, has a unique electronic band structure with the conic ''Dirac points'' at two inequivalent corners of the two-dimensional Brillouin zone. The electron mobility may be very high and lateral patterning with standard lithography methods allows device fabrication [1]. Two ways of obtaining graphene samples have been used up to now. In the first ''mechanical'' method, the carbon monolayers are mechanically split off the bulk graphite crystals and deposited onto a SiO_2/Si substrate [4]. This way an almost ''freestanding'' graphene is produced, since the carbon monolayer is practically not coupled to the substrate. The second method uses epitaxial growth of graphite on single-crystal silicon carbide (SiC). The ultrathin graphite layer is formed by vacuum graphitization [7] due to Si depletion of the SiC surface. This method has apparent technological advantages over the mechanical method; however, it does not guarantee that the carbon layer is electronically isolated from the substrate. Moreover, one expects a covalent coupling between both which may strongly modify the electronic properties of the overlayer. Yet, recent experiments show that the electronic properties of the interface are indeed dominated by the ultrathin carbon sheet, occasionally a graphene mono- or bilayer [1,2,6,8]. Most surprisingly, the electron spectrum of epitaxial graphene seems not to be affected by the substrate. However, the Fermi energy may be displaced from the Dirac point due to electron transfer from the substrate. For graphene grown on the Si-terminated SiC surface the Fermi level lies 0.45 eV above the conic point [5].

The graphene layers on both Si- or C-terminated SiC{0001} surfaces grow at temperatures above 1400 °C. The geometric structure of the interface is unclear. Forbeaux *et al.* [7] proposed that the graphene is loosely bound to the surface by van der Waals forces. On the contrary, combining STM with density-functional theory calculations Chen *et al.* [9] came to the conclusion that graphitization occurs on a complex 6×6 structure, although their LEED data indicate the $6\sqrt{3} \times 6\sqrt{3}R30°$ periodicity. On the C-terminated SiC$(000\bar{1})$ face, graphite growth on top of a 2×2 reconstruction was reported [7,10]. Berger *et al.* [1] and Hass *et al.* [2] observed high-quality graphene islands on 1×1 SiC$(000\bar{1})$, forming a $\sqrt{3} \times \sqrt{3}R30°$ interface structure. The most recent studies [5,8,11,12] converge to the conclusion that the graphene film rests on an intermediate carbon-rich underlayer.

In this Letter we address the graphene-SiC interface theoretically by employing *ab initio* density-functional theory calculations. We adopt the $\sqrt{3} \times \sqrt{3}R30°$ model assuming that the carbon-rich buffer layer is simply a carbon sheet that coherently fits the SiC surface (cf. Fig. 1). We find that the carbon layer is covalently bonded to the substrate. The binding energy overcompensates the elastic stress at the interface, making the covalent mechanism superior to the van der Waals bonding. We show that the coupling to the substrate removes the graphene-type electronic features from the energy region around the Fermi level. However, these features reappear with the second carbon layer placed atop the buffer sheet.

Our calculations were performed with the density-functional theory program package VASP [13–16] in the local spin density approximation (LSDA). Projector augmented wave pseudopotentials [17] were used. A special $7 \times 7 \times 1$ **k**-point sampling was applied for the Brillouin-zone integration. The plane wave basis set was restricted by a cutoff energy of 400 eV. We have chosen a $6H$-SiC polytype, which is most often used in experimental studies. The supercell was constructed of 6 bilayers of SiC, one or two carbon monolayers, and a vacuum interval needed to separate the slabs. The slab separation varied, depending on the carbon coverage, between 10 and 15 Å. The graphene layer was placed on the unreconstructed $6H$-SiC substrate such that the structure had a lateral $\sqrt{3} \times \sqrt{3}R30°$ elementary cell [Fig. 1(a)]. Because of the lattice mismatch of 8% between SiC and graphite, this requires an

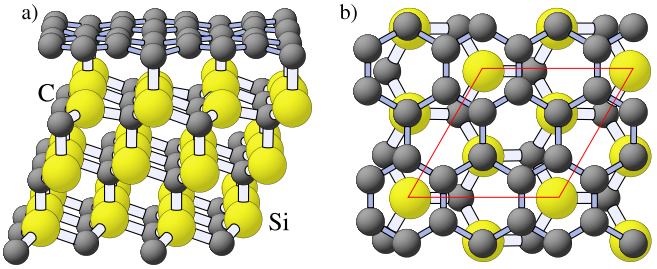

FIG. 1 (color online). Side view (a) and top view (b) of a graphene layer on the SiC(0001) surface. The $\sqrt{3} \times \sqrt{3}R30°$ surface unit cell is highlighted.

elastic adjustment at the interface. If the latter occurred exclusively via stretching the graphene layer, the elastic energy would amount to 0.8 eV per graphene unit cell. However, this energy is dramatically reduced when elastic relaxation of the substrate is taken into account (see below).

The interface unit cell [cf. Fig. 1(b)] contains three substrate surface atoms and four graphene unit cells. The dangling bonds of the substrate atoms at the cell corners remain unsaturated, while the other atoms bind to two carbon atoms of the hexagonal graphene ring. On the Si-terminated surface, we find an average graphene separation of 2.58 Å from the SiC substrate. The covalently bonded carbon atoms relax towards the SiC surface, such that the bond length is 2.0 Å. This is only slightly longer than the bond length 1.87 Å in SiC. The bonding releases 0.72 eV per graphene unit cell. For the C-terminated SiC$(000\bar{1})$ face, the graphene layer is somewhat closer (2.44 Å) to the substrate and the bond length of the carbon atoms reduces to 1.87 Å. The energy gain is 0.60 eV per graphene unit cell. For both interfaces, the substrate bonding atom relaxes outwards, whereas the partner graphene atom moves towards the substrate.

The stability of the considered interface is determined by the balance of the bonding energy and the elastic energy. Since the carbon layer is more rigid than the SiC crystal, the elastic stress should propagate into the substrate. To evaluate this effect we performed calculations for a graphene layer on two SiC bilayers, relaxing the lateral periodicity of the whole system. Indeed, the elastic energy dropped by more than 50% down to 0.38 eV (for the Si-terminated surface). For the net binding energy we have an estimate of 0.34 eV per graphene unit cell for the binding on the Si face and 0.2 eV for the C face. For a half-infinite substrate one expects a somewhat smaller number due to the propagation of the elastic deformation beneath the surface.

The proposed model contrasts the conventional adsorption picture, where the adsorbate adopts the lattice constant of the substrate. Yet, none of the common adsorbates would stay as a two-dimensional layer when separated from the substrate as graphene does. This signifies a strong interaction within the carbon layer, which prevails over the coupling to the surface. Calculating the total energy for larger separations (up to 5 Å) between the carbon sheet and the SiC substrate, we did not find a stable van der Waals bonded configuration.

For a second graphene layer placed in the graphite-type *AB* stacking, we find a weak bonding at a distance of 3.3 Å, very close to the bulk graphite value 3.35 Å. This conforms to the fact that LSDA, despite the lack of long-range nonlocal correlations, produces reasonable interlayer distances in van der Waals crystals like graphite [18,19] or *h*-BN [20]. As shown by Marini *et al.* [20], a delicate error cancellation between exchange and correlation underlies this apparent performance of the LSDA. The semilocal generalized gradient approximation, which violates this balance, fails to generate the interplanar bonding in both graphite [19] and *h*-BN [20], while producing a band structure identical to LSDA [19]. It is thus natural to assume that in our situation the bonding between the graphene layers is the same as in bulk graphite with the same interplanar distance. To reduce the calculational cost, we fixed the interplanar distance at this value.

The first graphene layer thus serves as a buffer between the SiC crystal and the van der Waals bonded second graphene sheet. Of course, the chosen interface structure (Fig. 1) is simplified. For a fully realistic calculation one should use the $6\sqrt{3} \times 6\sqrt{3}R30°$ unit cell, which almost exactly coincides with a 13×13 graphene cell and is thus commensurate with the graphene layer. Such a large unit cell is, however, computationally hardly tractable. The $6\sqrt{3} \times 6\sqrt{3}R30°$ interface, most often observed as a precursor of graphitization [3,7], is perhaps the most common realization of the buffer layer. Still, Berger *et al.* [1] found the graphene formation on a 1×1 C face leading to a $\sqrt{3} \times \sqrt{3}R30°$ interface just as depicted in Fig. 1. Capturing the covalent bonding mechanism, this model may provide the prototype electronic structure also for a more complex $6\sqrt{3} \times 6\sqrt{3}R30°$ interface.

Figures 2(a) and 2(b) show the electron energy spectrum of a single graphene layer on the two SiC surfaces. The shaded regions are the projected energy bands of SiC. The Kohn-Sham gap of 1.98 eV is smaller than the optical band gap (3.02 eV) of the bulk 6*H*-SiC, which is a common consequence of LSDA. The covalent bonding drastically changes the graphene electron spectrum at the Fermi energy. The ''Dirac cones'' are merged into the valence band, whereas the upper graphene bands overlap with the SiC conduction band, thus leaving a wide energy gap in the graphene spectrum. A similar gap opening due to hydrogen absorption on a single graphene sheet was predicted in Ref. [21]. The weakly dispersive interface states visible in Figs. 2(a) and 2(b) result from the interaction of the graphene layer with the three dangling orbitals of the substrate. Two of them make covalent bonds, while the third one in the center of the graphene ring remains unsaturated [cf. Fig. 1(b)]. A projection analysis of the wave functions reveals that the gap states close to the Fermi

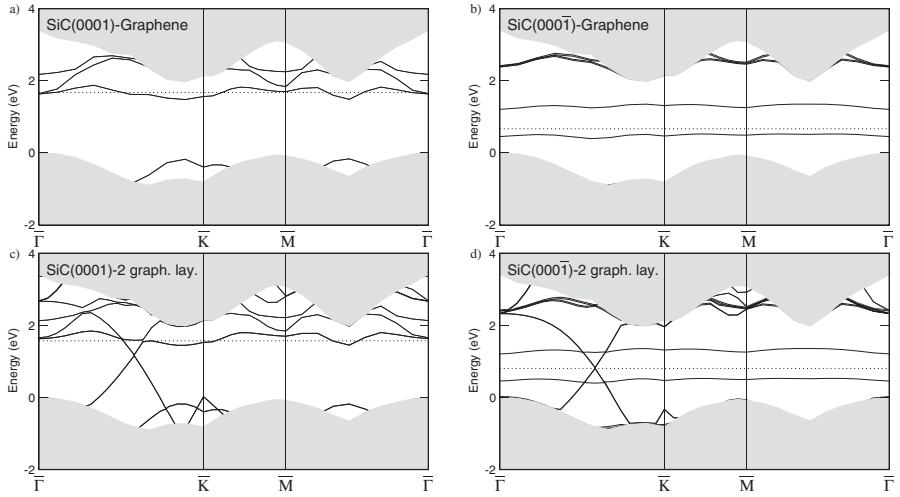

FIG. 2. Energy spectrum of the interface states of (a) the SiC(0001)-graphene interface, (b) the SiC(000$\bar{1}$)-graphene interface, (c) SiC(0001) with two layers of graphene, and (d) SiC(000$\bar{1}$) with two layers of graphene. The Fermi energy is indicated by the dashed line. $\bar{K}$ and $\bar{M}$ are the high-symmetry points of the surface Brillouin zone of the $\sqrt{3} \times \sqrt{3}R30°$ surface unit cell.

energy originate from the remaining dangling bonds of the substrate. On the Si face we find a half-filled metallic state, whereas on the C face the interface state is split into a singly occupied (spin polarized) and an empty state, making the interface insulating. In contrast, on both clean SiC surfaces LSDA predicts a substantial splitting of the surface states [0.86 eV for SiC(0001) and 0.45 eV for SiC(000$\bar{1}$); see Table I]. Actually, the gap between a singly occupied and an empty state is larger due to the Hubbard repulsion of the electrons (about 2 eV for the $\sqrt{3} \times \sqrt{3}R30°$ reconstructed surface [22,23]), but already LSDA correctly reproduces the insulating character of both surfaces.

The reason for the striking difference between the two graphene-covered surfaces becomes clear if one compares the planar localization of the two gap states. As seen in Fig. 3(a) for the Si face, the interface state electron density is strongly delocalized. The projection analysis shows that this results from the hybridization with graphene-induced electron states overlapping with the conduction band [see Fig. 2(a)]. Given the delocalized nature of the interface state, we expect the influence of Hubbard correlations to be small. In contrast, at the C-terminated substrate the electron state retains its localized character, although it is smeared over a carbon ring just above the unsaturated C-dangling bond. The localization favors the spin polarization and thus the splitting of the gap state, whereas the interface state at the Si face remains spin degenerate. In the former case, Hubbard correlations may lead to a further splitting of the interface state.

Figures 2(c) and 2(d) show that the second carbon layer possesses an electronic structure similar to freestanding graphene. The characteristic conic point appears on the $\bar{\Gamma} - \bar{K}$ line (note that since the Brillouin zone corresponds to the $\sqrt{3} \times \sqrt{3}R30°$ unit cell, the conic point is not located at the $\bar{K}$ point). The narrow interface band has not been seen in photoemission [5,6], possibly because the interface state is buried under two graphene layers. The metallic interface state on the Si-terminated substrate pins the Fermi level just above the conic point, making the second graphene layer n doped. Recent STM measurements [8] reveal the existence of such an interface state. The Dirac point lies 0.4 eV below the Fermi level, in good agreement with the results of Bostwick *et al.* [5]. On C-terminated

TABLE I. Parameters of the unreconstructed and graphene-covered SiC{0001} surfaces in eV: work function ϕ, positions of the occupied and the unoccupied surface and interface states above the valence band edge (E_o, E_u) and their corresponding bandwidths (B_o, B_u).

	Work function ϕ	E_o	B_o	E_u	B_u
SiC(0001) 1×1	4.75	$E_v + 0.92$	0.45	$E_v + 1.78$	0.53
SiC(0001)-graphene	3.75	$E_v + 1.64$	0.35	—	—
SiC(0001)-graphene	4.33	$E_v + 1.64$	0.40	—	—
SiC(000$\bar{1}$) 1×1	5.75	$E_v + 0.05$	0.75	$E_v + 0.50$	0.45
SiC(000$\bar{1}$)-graphene	5.33	$E_v + 0.43$	0.13	$E_v + 1.19$	0.14
SiC(000$\bar{1}$)-2 graphene	5.31	$E_v + 0.44$	0.10	$E_v + 1.19$	0.15
Graphene (single layer)	5.11				

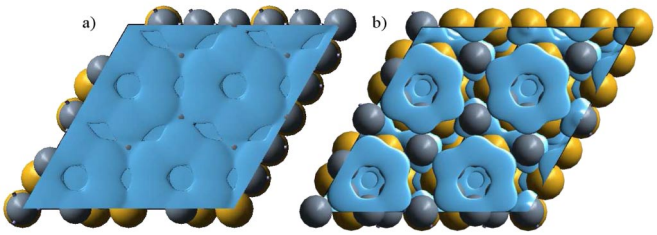

FIG. 3 (color online). Charge density of the interface states at the Fermi energy for a single graphene layer on (a) SiC(0001) and (b) SiC(000$\bar{1}$).

substrate the Fermi level runs exactly through the conic point. Hence the interface is semimetallic just as for freestanding graphene. This was indeed observed for a graphene-covered C face by Berger *et al.* [1].

The parameters of the electron states for the different interfaces are summarized in Table I. For clean unreconstructed surfaces we find work functions of 4.75 eV (Si-terminated surface) and 5.75 eV (C-terminated surface). The former value is practically the same as the work function of the reconstructed SiC(0001) [24]. The first graphene layer reduces this value to 3.75 eV, which is 1.3 eV lower than the work function of freestanding graphene. The drastic reduction of the work function is caused by a charge flow from graphene to the interface region, which induces a dipole layer. On the C face the graphene overlayer also reduces the work function, but to a lesser extent such that it remains above the graphene value. Adding the second graphene layer makes the work function closer to that of freestanding graphene for both faces.

The Fermi level pinning close to the conduction band makes the graphitized Si face especially suitable for Ohmic contacts on *n*-type SiC because it guarantees a low Schottky barrier. Indeed, Lu *et al.* [25] find a very low resistance for thermally treated SiC contacts with nickel and cobalt, while other metals, which form carbides and thereby remove the graphitic inclusions, were rectifying. Seyller *et al.* measured the Schottky barrier between *n*-type 6*H*-SiC(0001) and graphite by photoelectron spectroscopy and found a low value of 0.3 eV [26]. On the contrary, for the C-terminated face the Fermi level is close to the middle of the band gap.

In conclusion, we have shown that even when the first carbon layer on SiC is kept in its ''perfect'' graphene geometry (which is practically the case in our interface model) it does not manifest the electronic structure of freestanding graphene. It is apparent that any possible interface defects cannot ''restore'' the electron spectrum to that of freestanding graphene. The graphene overlayers on SiC(0001) and SiC(000$\bar{1}$) possess qualitatively different electronic structures. While the former is metallic, the latter is semiconducting. The Dirac cones in the electron spectrum appear only with the second carbon layer. The first carbon sheet acts as a buffer layer between a covalent SiC crystal and a van der Waals bonded stack of graphene layers.

This work was supported by Deutsche Forschungsgemeinschaft within the SiC Research Group.

*Alexander.Mattausch@physik.uni-erlangen.de

[1] C. Berger *et al.*, Science **312**, 1191 (2006).
[2] J. Hass, C. A. Jeffrey, R. Feng, T. Li, X. Li, Z. Song, C. Berger, W. A. de Heer, P. N. First, and E. H. Conrad, Appl. Phys. Lett. **89**, 143106 (2006).
[3] T. Seyller *et al.*, Surf. Sci. **600**, 3906 (2006).
[4] Y. Zhang, Z. Jiang, J. P. Small, M. S. Purewal, Y.-W. Tan, M. Fazlollahi, J. D. Chudow, J. A. Jaszczak, H. L. Stormer, and P. Kim, Phys. Rev. Lett. **96**, 136806 (2006).
[5] A. Bostwick, T. Ohta, T. Seyller, K. Horn, and E. Rotenberg, Nature Phys. **3**, 36 (2007).
[6] T. Ohta, A. Bostwick, T. Seyller, K. Horn, and E. Rotenberg, Science **313**, 951 (2006).
[7] I. Forbeaux, J.-M. Themlin, and J.-M. Debever, Phys. Rev. B **58**, 16 396 (1998).
[8] P. Mallet, F. Varchon, C. Naud, L. Magaud, C. Berger, and J.-Y. Veuillen, Phys. Rev. B **76**, 041403(R) (2007).
[9] W. Chen, H. Xu, L. Liu, X. Gao, D. Qi, G. Peng, S. C. Tan, Y. Feng, K. P. Loh, and A. T. S. Wee, Surf. Sci. **596**, 176 (2005).
[10] I. Forbeaux, J.-M. Themlin, A. Charrier, F. Thibaudau, and J.-M. Debever, Appl. Surf. Sci. **162**, 406 (2000).
[11] J. Hass, R. Feng, J. E. Millán-Otoya, X. Li, M. Sprinkle, P. N. First, C. Berger, W. A. de Heer, and E. H. Conrad, Phys. Rev. B **75**, 214109 (2007).
[12] F. Varchon *et al.*, arXiv:cond-mat/0702311 [Phys. Rev. Lett. (to be published)].
[13] G. Kresse and J. Hafner, Phys. Rev. B **47**, 558 (1993).
[14] G. Kresse, Ph.D., thesis, Technische Universität Wien, Austria, 1993.
[15] G. Kresse and J. Furthmüller, Phys. Rev. B **54**, 11 169 (1996).
[16] G. Kresse and J. Furthmüller, Comput. Mater. Sci. **6**, 15 (1996).
[17] G. Kresse and D. Joubert, Phys. Rev. B **59**, 1758 (1999).
[18] J.-C. Charlier, X. Gonze, and J. P. Michenaud, Carbon **32**, 289 (1994).
[19] N. Ooi, A. Rairkar, and J. B. Adams, Carbon **44**, 231 (2006).
[20] A. Marini, P. García-González, and A. Rubio, Phys. Rev. Lett. **96**, 136404 (2006).
[21] E. J. Duplock, M. Scheffler, and P. J. D. Lindan, Phys. Rev. Lett. **92**, 225502 (2004).
[22] M. Rohlfing and J. Pollmann, Phys. Rev. Lett. **84**, 135 (2000).
[23] V. I. Anisimov, A. E. Bedin, M. A. Korotin, G. Santoro, S. Scandolo, and E. Tosatti, Phys. Rev. B **61**, 1752 (2000).
[24] M. Wiets, M. Weinelt, and T. Fauster, Phys. Rev. B **68**, 125321 (2003).
[25] W. Lu, W. C. Mitchel, G. R. Landis, T. R. Crenshaw, and W. E. Collins, J. Appl. Phys. **93**, 5397 (2003).
[26] T. Seyller, K. V. Emtsev, F. Speck, K.-Y. Gao, and L. Ley, Appl. Phys. Lett. **88**, 242103 (2006).